$O(N)$ matrix-vector multiplication in periodic MoM

Denis Tihon
ICTEAM institute
Université catholique de Louvain
Louvain-la-Neuve, Belgium
denis.tihon@uclouvain.be

Christophe Craeye
ICTEAM institute
Université catholique de Louvain
Louvain-la-Neuve, Belgium
christophe.craeye@uclouvain.be

***Abstract*—Using the periodic Green's function, periodic structures can be simulated with the Method of Moments. In classical implementation, first the periodic impedance matrix of the structure is filled. Then, it is inverted. The computational complexity of these steps scale as $O(N^2)$ and $O(N^3)$, respectively, with N the number of basis and testing functions used to discretize the geometry. When dealing with large structures, iterative techniques are preferred due to their lower complexity, which ranges between $O(N)$ and $O(N \log N)$. In this paper, we propose an algorithm for matrix-vector multiplication that is specialized for the simulation of elongated structures and scales as $O(N)$. The algorithm is based on a plane wave decomposition of the fields. The peculiarity of the proposed algorithm and its efficiency lies in the proper ordering of the operations performed. The complexity of the method is validated through the simulation of an array of dielectric nanowires of various sizes.**

***Index Terms*—Periodic Method of Moments, iterative solver**

I. Introduction

The simulation of periodic structures has been studied for a long time in the context of photonic crystals [1], reflectarrays [2], metamaterials [3], [4] and metasurfaces [5]. As a particular case, the simulation of periodic elongated structures, such as the wire medium, can find applications in the design of imaging systems [3], absorbing surfaces [4], [6] or radiative heat transfer [7].

Periodic structures illuminated by a quasi-periodic excitation, i.e. an excitation that is periodic within a linear phase shift, can be simulated using the periodic Method of Moments (MoM) [1], [2], [8]–[10], [12]–[15]. Classically, the method is decomposed into two steps. First, the impedance matrix of the structure is computed. Then, the resulting system of equations is solved. Noting N the number of unknowns, the computational complexity of the first step scales as $O(N^2)$, while the second one scales as $O(N^3)$. Studying large geometries, iterative techniques are preferred due to their lower complexities [1], [8]–[10]. Using these techniques, the impedance matrix does not need to be computed entirely and the matrix-vector multiplication is accelerated, reducing the time and memory consumption. These methods are based on the fact that far-field interactions can be computed using low-rank operators. First, the fields emitted by the currents are expanded using a limited set of functions (polynomials evaluated through interpolation between sampling points [10], multipoles [1], [9] or Cartesian expansion [8]). Once the fields have been computed, they are projected onto the testing functions, providing an asymptotic complexity ranging from $O(N)$ to $O(N \log N)$, depending on the way the number of unknowns is increased: increasing mesh density, increasing unit cell lateral dimensions, increasing unit cell height. In the latter case, complexity scales as $O(N \log N)$.

In this paper, we propose an algorithm for fast matrix-vector multiplication that is specialized for elongated periodic structures. It scales as $O(N)$ provided that the increase in the number of unknowns is originating from an increase in the height of the unit cell. While available methods tend to separate into two consecutive steps, the convolution of the Green's function with the currents and the projection of the resulting fields on the testing functions, the proposed method treats the two problems simultaneously. It is shown that, constraining the order in which the operations are performed, the complexity is decreased from $O(N \log N)$ to $O(N)$.

The presented method is based on the fact that one unit cell of the periodic structure can be considered as a waveguide with quasi-periodic boundary conditions, with waveguide modes corresponding to plane waves of a given Floquet family. The field on any testing function (TF) within this waveguide can be decomposed into three contributions: the contribution of basis functions (BF) located above the TF, which can be computed using downward propagating and evanescent plane waves, the contribution of the BF located below the TF, which can be computed using upward propagating and evanescent plane waves, and the contribution of BF located close by, which can be computed explicitly using for instance the periodic Green's function [13]–[15]. The core of the proposed method lies in the treatment of the intermediate-to-far-field interactions.

The remainder of this paper is organized as follows. In Section II, the plane-wave formalism used to compute the interaction between BF and TF is described. Section III focuses on the numerical implementation of the formalism. It is shown how the operations should be sorted to reach an $O(N)$ complexity. In Section IV, the asymptotic complexity of the method is illustrated by simulating a periodic array of dielectric wires with varying lengths.

II. Plane wave decomposition of the fields

Consider a structure periodic along two directions, called $\hat{\mathbf{x}}$ and $\hat{\mathbf{y}}$, with periodicities of a and b, respectively. For the sake of simplicity, we will consider the case where $\hat{\mathbf{x}}$ and $\hat{\mathbf{y}}$ are perpendicular. However, the non-perpendicular case can be

978-1-7281-0563-5/19/$31.00 ©2019 IEEE

treated by adapting the family of plane waves considered to expand the fields. We define the vertical direction $\hat{\mathbf{z}} = \hat{\mathbf{x}} \times \hat{\mathbf{y}}$. The interactions between a periodically replicated BF and a TF through a medium of arbitrary permittivity ε and permeability μ at an angular frequency ω can be formulated as a sum of plane wave contributions provided that the BF and TF are separated by a minimum distance $\Delta_z > 0$ in the $\hat{\mathbf{z}}$ direction. Plane wave i is characterized by a wave vector $\mathbf{k}_i = (k_{x,i}, k_{y,i}, s\gamma_i)$ such that

$$k_{x,i} = \frac{\phi_x}{a} + m_i \frac{2\pi}{a}, \tag{1}$$

$$k_{y,i} = \frac{\phi_y}{b} + n_i \frac{2\pi}{b}, \tag{2}$$

$$\gamma_i = \pm\sqrt{k^2 - k_{x,i}^2 - k_{y,i}^2}, \tag{3}$$

with $k^2 = \omega^2 \varepsilon \mu$ the wavenumber, ϕ_x and ϕ_y the phase shifts between consecutive replicas of the BF in the $\hat{\mathbf{x}}$ and $\hat{\mathbf{y}}$ directions, respectively, m_i and n_i two integers and $s = 1$ if the BF is located below the TF and $s = -1$ otherwise. The sign of γ in (3) is chosen such that its argument is lying in the $]-\pi; 0]$ interval.

In order to simplify the calculations, we introduce a specialized system of coordinates for each plane wave [11]:

$$\hat{\mathbf{e}}_i = \frac{1}{k_{t,i}}\Big(-k_{y,i}, k_{x,i}, 0\Big), \tag{4}$$

$$\hat{\mathbf{m}}_i = -\frac{s\gamma_i}{k_{t,i}k}\Big(k_{x,i}, k_{y,i}, -\frac{sk_{t,i}^2}{\gamma_i}\Big), \tag{5}$$

$$\hat{\mathbf{k}}_i = \frac{1}{k}\Big(k_{x,i}, k_{y,i}, s\gamma_i\Big), \tag{6}$$

with $k_{t,i} = \sqrt{k_{x,i}^2 + k_{y,i}^2}$. Using this system of coordinates, the electric and magnetic fields generated on the TF by electric currents on the BF, respectively Z^{EJ} and Z^{HJ}, read [12]

$$\begin{aligned} Z^{EJ} = \sum_i \frac{\eta k}{ab2\gamma_i}\Big(&\tilde{f}_{b,e}(-\mathbf{k}_i)\tilde{f}_{t,e}(\mathbf{k}_i) \\ &+ \tilde{f}_{b,m}(-\mathbf{k}_i)\tilde{f}_{t,m}(\mathbf{k}_i)\Big), \end{aligned} \tag{7}$$

$$\begin{aligned} Z^{HJ} = \sum_i \frac{k}{ab2\gamma_i}\Big(&\tilde{f}_{b,m}(-\mathbf{k}_i)\tilde{f}_{t,e}(\mathbf{k}_i) \\ &- \tilde{f}_{b,e}(-\mathbf{k}_i)\tilde{f}_{t,m}(\mathbf{k}_i)\Big), \end{aligned} \tag{8}$$

with $\eta = \sqrt{\mu/\varepsilon}$ the impedance of the medium, $\tilde{\mathbf{f}}_b(\mathbf{k}_i)$ and $\tilde{\mathbf{f}}_t(\mathbf{k}_i)$ the Fourier transforms of the BF and TF, respectively, $f_{j,e}(\mathbf{k}_i) = \mathbf{f}_j(\mathbf{k}_i) \cdot \hat{\mathbf{e}}_i$ and $f_{j,m}(\mathbf{k}_i) = \mathbf{f}_j(\mathbf{k}_i) \cdot \hat{\mathbf{m}}_i$.

Since the BF and TF are separated by a distance $\Delta_z > 0$, the sum converges exponentially, so that it can be truncated. The number of terms C required to reach a relative error θ asymptotically depends on the ratio $\Delta_z^2/(ab)$ following the law

$$C \propto \frac{-\ln^2(\theta)ab}{\Delta_z^2}. \tag{9}$$

It illustrates the rank-limited nature of distant interactions: there are only few degrees of freedom left, so that the computations can be accelerated for distant interactions.

III. Fast matrix-vector multiplication

The fast matrix-vector multiplication is based on the classification of the interactions between BF and TF into three classes. The upward interactions, for which the BF is located "sufficiently" far below the TF, the downward interactions, for which the BF is located "sufficiently" far above the TF, and the near-field interactions, which consist of the rest. A BF is considered to be "sufficiently" far if the minimum distance between the BF and TF is higher than a predefined threshold. The higher the threshold, the larger the near-field zone and the lower the number of terms C needed to reach a given accuracy for far-field interactions.

A. Far-field interactions

For illustration purposes, we will focus our explanation on one upward mode. The extension to any number of upward or downward mode(s) is straightforward. Consider a TF k whose vertical position, defined as the vertical position of its lowest point, is z'_k. We define the position z_j of BF j as the position of its highest point. We impose a threshold Δ such that, if the distance $z'_k - z_j$ between a BF j and a TF k is smaller than the threshold, the interaction is considered as a near-field interaction and is computed separately. Then, the contribution of upward mode i to the electric and magnetic fields tested on TF k, designated as $b_{k,i}^E$ and $b_{k,i}^H$ respectively, read

$$b_{k,i}^E = \eta\big(E_i^e(z'_k, -\infty)\tilde{f}'_{k,e}(\mathbf{k}_i) + E_i^m(z'_k, -\infty)\tilde{f}'_{k,m}(\mathbf{k}_i)\big) \tag{10}$$

$$b_{k,i}^H = E_i^e(z'_k, -\infty)\tilde{f}'_{k,m}(\mathbf{k}_i) - E_i^m(z'_k, -\infty)\tilde{f}'_{k,e}(\mathbf{k}_i) \tag{11}$$

with

$$\begin{aligned} E_i^e(z_2, z_1) &= \frac{k}{ab2\gamma_i} \\ &\times \sum_{\{j|z_1-\Delta<z_j<z_2-\Delta\}} \Big(x_j^J \tilde{f}_{j,e}(-\mathbf{k}_i) + x_j^M \tilde{f}_{j,m}(-\mathbf{k}_i)\Big), \end{aligned} \tag{12}$$

$$\begin{aligned} E_i^m(z_2, z_1) &= \frac{k}{ab2\gamma_i} \\ &\times \sum_{\{j|z_1-\Delta<z_j<z_2-\Delta\}} \Big(x_j^J \tilde{f}_{j,m}(-\mathbf{k}_i) - x_j^M \tilde{f}_{j,e}(-\mathbf{k}_i)\Big). \end{aligned} \tag{13}$$

x_j^J and x_j^M represent the amplitude associated to the electric and magnetic currents on BF j, respectively. E_i^e physically corresponds to the amplitude of the TE plane wave with wave-vector $\mathbf{k}_i$ reaching the TF, while E_i^m corresponds to the amplitude of the TM plane wave.

If the field is first computed on the lowest TF, the E_i^e and E_i^m terms previously computed can be reused for TFs located above. Indeed, provided that the fields have already been computed for TF k and should now be computed for TF k' such that $z'_k < z'_{k'}$, one can write

$$E_i^e(z'_{k'}, -\infty) = E_i^e(z'_k, -\infty) + E_i^e(z'_{k'}, z'_k), \tag{14}$$

$$E_i^m(z'_{k'}, -\infty) = E_i^m(z'_k, -\infty) + E_i^m(z'_{k'}, z'_k). \tag{15}$$

Numerically, it means that the $E_i^{e/m}$ terms can be computed incrementally and then projected on successive TF.

To implement this algorithm, the position of the BF and TF, as defined previously, are computed and the BF and TF are sorted accordingly. Then, the vertical position is varied continuously. Each time a BF is crossed, its contribution is added to the mode considered using Equations (12) and (13). Each time a TF is crossed, the contribution of the mode to the total fields on that TF is added using Equations (10) and (11). In order to enforce the minimum distance Δ between BF and TF and thus limit the number of modes that should be considered, the positions of the TF are decreased by the corresponding amount before comparing the position of the BF and TF. Doing so, all the far-field interactions are computed with a complexity $O(CN)$, C corresponding to the number of modes used to expand the fields. For fixed unit cell lateral dimensions, C is constant.

B. Near-field interactions

As explained in the introduction, the near-field interactions are computed using the code of [14]. The corresponding impedance matrix is banded-diagonal, so that the filling time and the matrix-vector multiplication time scale as $O(N)$. It should be noted that this kind of matrices can be rapidly LU-decomposed and that decomposition remains banded-diagonal. The latter fact can be used for preconditioning.

C. General notes about the method

A first interesting note concerns the disappearance of the $\log(N)$ factor in the complexity. During the preparation step, the BF and TF are sorted according to their position. Sorting a list of N elements can be accomplished with a complexity of $O(N \log N)$. Therefore, the usual $O(N \log N)$ complexity has not been fully eliminated, but has been transferred to the pre-processing step of the method. However, the constant factor associated to the sorting algorithm is so small that the time required to sort the BF and TF is truly negligible compared to the rest of the method.

Another interesting note concerns the generality of the method. While it is well suited for periodic structures thanks to the limited cross-section of the unit cell, it can be adapted to non-periodic structures provided that

1) One can find a modal decomposition of the fields based on homogeneous solutions to Maxwell's equations.
2) The amplitude of each mode is known at a given location, *e.g.* thanks to causality.
3) The spatial variation of the amplitude of the modes due to currents can be computed.

One could imagine applying this algorithm with cylindrical or spherical wave expansions originating from different locations. However, the total number of modes would probably not be as low as in the periodic case, limiting the efficiency of the method in practice.

IV. Numerical Results

In order to validate the method, we studied an array of free-standing dielectric wires [16] of varying lengths. The wires are arranged in a square lattice with a periodicity of 420 nm. The diameter of the wires is 300 nm and their length ranges from 500 nm to 50 μm. The wavelength is 2 μm. The material constituting the wires has a relative permittivity of 10.

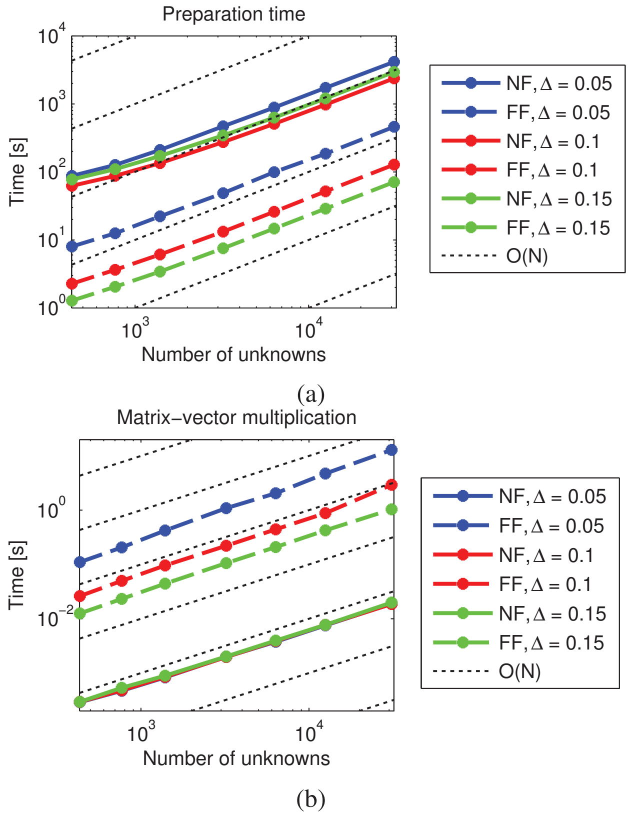

Fig. 1. (a) Preparation time and (b) matrix-vector multiplication time as a function of the number of unknowns.

We tested the algorithm with different near-field thresholds ($\Delta = 21, 42, 63$ nm) and for varying wire length ($L = 0.5, 1, 2, 5, 10, 20$ and 50 μm) and therefore varying number of unknowns ($N = 432, 768, 1392, 3216, 6336, 12528$ and 31056). The numbers of modes were chosen to reach an error $\theta = 10^{-3}$ (cf. Equation (9)) The wires were meshed with RWG [17], rooftop and hybrid basis functions. The code was run on a laptop with a Intel i3-4000M CPU. The results can be seen in Fig. 1. In Fig. 1(a), the preparation time is shown for the near-field and far-field interactions. Near-field interactions consist in computing the impedance matrix entries for near-field interactions, while the far-field preparation consists in computing the Fourier transform of the BF and TF for each mode. In Fig. 1(b), the time required for one matrix-vector multiplication is shown. The time devoted to the near-field and far-field interactions is shown separately. Note that, for each iteration, the interactions between the BFs and TFs are computed through the air as well as through the dielectric medium. The linear complexity is clearly visible from the graphs.

V. Conclusion

We presented an algorithm for the fast matrix-vector multiplication in periodic MoM. The method is well suited for the iterative solution of elongated structures, such as a wire medium. It is based on separating upward and downward plane-wave interactions and on constantly updating the plane-wave amplitudes and their projections, as the observer moves vertically. It is shown that, by modifying the order in which operations are carried out, it is possible to reduce the complexity to reach a linear asymptotic behaviour. The theoretical complexity is confirmed through numerical examples.

References

[1] Y. Otani and N. Nishimura, "A periodic FMM for Maxwell's equations in 3D and its applications to problems related to photonic crystals," *Journal of Computational Physics*, Vol. 227, no. 9, pp. 4630-4652, 2008.

[2] R. Florencio, R.R. Boix and J.A. Encinar, "Enhanced MoM analysis of the scattering by periodic strip grating in multilayered substrates," *IEEE Transactions on Antennas and Propagation*, Vol. 61, no. 10, pp. 5088-5099, 2013.

[3] P.A. Belov, Y. Hao and S. Sudhakaran, "Subwavelength microwave imaging using an array of parallel conducting wires as a lens," *Physical Review B*, Vol. 73, no. 3, pp. 033108, 2006.

[4] E.E. Narimanov, H. Li, Y.A. Barnakov and M.A. Noginov, "Darker than black: radiation-absorbing metamaterial," in *Optical Society of America, Quantum Electronics and Laser Science Conference*, pp. QPDA6, 2010.

[5] G. Minatti *et al.*, "Modulated metasurface antenna for space: synthesis, analysis and realization," *IEEE Transactions on Antennas and Propagation*, Vol. 63, no. 4, pp. 1288-1300, 2015.

[6] K. Mizuno *et al.*, "A black body absorber from vertically aligned singe-walled carbon nanotubes," *Proceedings of the National Academy of Science*, Vol. 106, no. 15, pp. 6044-6047, 2009.

[7] C. Simovski, S. Maslovski, I. Nefedov and S. Tretyakov, "Optimization of radiative heat transfer in hyperbolic metamaterials for thermophotovoltaic applications," *Optics express*, Vol. 21, no. 12, pp. 14988-15013, 2013.

[8] A.D. Baczewski, D.L. Dault and B. Shanker, "Accelerated Cartesian Expansions for the rapid solution of periodic multiscale problems," *IEEE Transactions on Antennas and Propagation*, Vol. 60, no. 9, pp. 4281-4290, 2012.

[9] M. Wei and W.C. Chew, "A broadband ML-FMA for 3-D periodic Green's function in 2-D lattice using Ewald summation," *IEEE Transactions on Antennas and Propagation*, Vol. 65, no. 6, pp. 3134-3145, 2017.

[10] S. Li, D.A. Van Orden and V. Lomakin, "Fast periodic interpolation method for periodic unit cell problems," *IEEE Transactions on Antennas and Propagation*, Vol. 58, no. 12, 2010.

[11] K. Alkhalifeh, G. Hislop, N.A. Ozdemir and C. Craeye, "Efficient MoM simulation of 3-D antennas in the vicinity of the ground," *IEEE Transactions on Antennas and Propagation*, Vol. 64, no. 12, pp. 5335-5344, 2016.

[12] D. Tihon and C. Craeye, "Fast computation of the impedance matrix for the periodic Method of Moments using a plane wave decomposition," *IEEE 10th European Conference on Antennas and Propagation (EuCAP)*, pp. 1-4, 2016.

[13] C. Craeye, X. Radu, A. Schuchinsky and F. Capolino, "Fundamentals of Method of Moments for metamaterials," in *Theory and Phenomena of Metamaterials*, CRC Press, 2009.

[14] X. Dardenne and C. Craeye, "Method of Moments simulation of infinitely periodic structures combining metal with connected dielectric objects," *IEEE Transactions on Antennas and Propagation*, Vol. 56, no. 8, pp. 2372-2380, 2008.

[15] S. Oroskar, D.R. Jackson and D.R. Wilton, "Efficient computation of the 2D periodic Green's function using the Ewald method," *Journal of Computational Physics*, Vol. 219, no. 2, pp. 899-911, 2006.

[16] N.A. Ozdemir and C. Craeye, "Efficient integral equation-based analysis of finite periodic structures in the optical frequency range," *Journal of Optical Society of Americal A*, Vol. 30, no. 12, pp. 2510-2518, 2013.

[17] S. Rao, D. Wilton and A. Glisson, "Electromagnetic scattering by surfaces of arbitrary shapes," *IEEE Transactions on Antennas and Propagation,* Vol. 30, no. 3, pp. 409-418, 1982.